On the ability of OMIP models to simulate the ocean mixed layer depth and its seasonal cycle in the Arctic Ocean

Allende S. [1, *], Fichefet T. [1], Goosse H. [1], Treguier Anne-Marie [2]

[1] Earth and Climate Research, Earth and Life Institute, Université catholique de Louvain, Louvain-la-Neuve, Belgium
[2] Univ Brest, CNRS, IRD, Ifremer, Laboratoire d'océanographie physique et spatiale, IUEM, 29280, Plouzané, France

* Corresponding author : S. Allende, email address : sofia.allende@uclouvain.be

Abstract :

We evaluate the skills of ocean–sea ice general circulation models involved in the Ocean Modeling Intercomparison Project in simulating the ocean mixed layer depth and its seasonal cycle in the Arctic region. During summer months, all models consistently underestimate the mixed layer depth compared to observational data from the Monthly Isopycnal Mixed layer Ocean Climatology and the Ice Tethered Profilers. In fall and winter, the models exhibit great variability compared to observational data, and inter-model comparison reveals differences up to several tens of meters. We analyze the origin of the fall and winter model biases in ice-covered regions, where the seasonal cycle of the surface salinity and mixed layer depth is strongly influenced by brine rejection resulting from ocean–sea ice interactions.

Focusing first on the central Arctic Ocean, defined here as the region north of 80 N, we show that all models simulate more or less the same vertical sea ice mass balance and thus similar salt fluxes into the ocean during sea ice freezing. Furthermore, the model ensemble features a strong relationship between the stratification profile in September and the mixed layer depth at the end of winter. The models whose stratification compares the best to observational data also display the most realistic values of the mixed layer depth at the end of winter. We argue that the discrepancies between models are therefore not so much linked to the surface salt balance but rather to the accuracy with which those models reproduce the vertical salinity profile. In short, a weakly stratified ocean tends to create a deep mixed layer, while strong stratification leads to a shallow mixed layer. To substantiate this conclusion, we apply a simple conceptual model, which simulates the month-to-month evolution of the mixed layer depth using as input the vertical salinity gradients and the surface salt fluxes from general circulation models. Quite surprisingly, this simplified dynamics captures very well the behavior of the general circulation models, emphasizing the role of the different vertical stratification in the control of the mixed layer depth. Furthermore, this interplay may also significantly account for the large mixed layer biases observed in other ice-covered regions of the pan-Arctic seas, even though sea–ice ocean interaction is not the only driver of mixed layer variability in fall and winter there.

Highlights

► Large biases in the fall and winter mixed layer depth are present in ocean models. ► OMIP models simulate similar salt fluxes into the ocean during sea ice freezing. ► A simple model of the ice-ocean salt flux captures much of OMIP mixed layer depth.

Keywords : Mixed layer depth, Arctic ocean, Sea ice, Ocean stratification, OMIP models

1. Introduction

The Arctic mixed layer (ML) is the upper layer of the Arctic Ocean that controls the exchanges between the deeper ocean, sea ice and the atmosphere. Those transfers are influenced by complex thermodynamical and dynamical processes likely to create strong heterogeneities in ocean surface properties, such as discontinuous and dynamic sea ice cover, ocean eddies, or salinity fronts and filaments at the kilometre-scale (Rippeth and Fine, 2022; Goosse et al., 2018; Horvat et al., 2016). The ML is characterized by a homogeneous density profile, which goes from the oceanic surface to the beginning of the pycnocline. An accurate characterisation of the mixed layer depth (MLD) is relevant to a large number of physical and biological processes. From a physical point of view, the ML mediates the transfer of heat between ocean, sea ice and atmosphere, and therefore plays a key role in the global energy budget and oceanic circulation (McPhee, 2008; Gettelman and Rood, 2016). In the last decades, global climate change has strongly affected the Arctic region, in particular leading to a fast decrease in sea ice extent (Timmermans and Marshall, 2020; Nummelin et al., 2016; Perovich and Richter-Menge, 2009). This retreat of the sea ice affects the dynamics of the ML. From a biological point of view, a major spatial expansion of under-ice phytoplankton blooms at high latitudes has been observed by Arrigo et al. (2012), Boles et al. (2020) and Horvat et al. (2017). These organisms benefit from the mixing in the upper layer of the ocean (Ardyna et al., 2020).

On the ability of OMIP models to simulate the ocean mixed layer depth and its seasonal cycle in the Arctic Ocean

Model name	Phase	Spatial resolution	Vertical resolution	OM	SIM	VMS
CAS-ESM2-0 Dong et al. (2021)	OMIP-I	tripolar 1°	30 layers	LICOM3	CICE4	One-Point Closure Model Canuto et al. (2001, 2002)
CESM2 Danabasoglu et al. (2020)	OMIP-I	dipolar 1°	60 layers	POP2	CICE5	K-Profile Parameterization Li et al. (2016)
CMCC-CM2-SR5 Cherchi et al. (2019)	OMIP-I	ORCA-1°	50 layers	NEMO3.6	CICE4	Turbulent kinetic energy scheme Blanke and Delecluse (1993)
CMCC-ESM2 Lovato et al. (2022)	OMIP-I	ORCA-1°	50 layers	NEMO3.6	CICE4	Turbulent kinetic energy scheme Blanke and Delecluse (1993)
IPSL-CM6A-LR Boucher et al. (2020)	OMIP-I	eORCA-1°	75 layers	NEMO-OPA	LIM3	Turbulent kinetic energy scheme Blanke and Delecluse (1993)
MRI-ESM2-0 Yukimoto et al. (2019)	OMIP-I	tripolar 1° ×(0.3 − 0.5)°	60 layers	MRI.COMv4	MRI.COMv4	Length scale scheme Umlauf and Burchard (2003)
CESM2 Danabasoglu et al. (2020)	OMIP-II	dipolar 1°	60 layers	POP2	CICE5	K-Profile Parameterization Li et al. (2016)
CMCC-CM2-HR4 Cherchi et al. (2019)	OMIP-II	ORCA-0.25°	50 layers	NEMO3.6	CICE	Turbulent kinetic energy scheme Blanke and Delecluse (1993)
CMCC-CM2-SR5 Cherchi et al. (2019)	OMIP-II	ORCA-1°	50 layers	NEMO3.6	CICE4	Turbulent kinetic energy scheme Blanke and Delecluse (1993)
MRI-ESM2-0 Yukimoto et al. (2019)	OMIP-II	tripolar 1° ×(0.3 − 0.5)°	60 layers	MRI.COMv4	MRI.COMv4	Length scale scheme Umlauf and Burchard (2003)

Table 1
Brief description of the OMIP models used in our study, featuring their name, associated OMIP phase, spatial resolution, vertical resolution, underlying ocean (OM) and sea ice models (SIM) and the vertical mixing scheme (VMS).

While crucial, an accurate modeling of the MLD remains a challenge for global climate models. In particular, large discrepancies are found among the climate models that performed climate projections for the assessment reports of the Intergovernmental Panel on Climate Change (IPCC) (Cassotta et al., 2022; Meredith et al., 2019). Previous studies by Ilıcak et al. (2016) and Tsujino et al. (2020) highlighted the poor skills of general circulation models (GCM) in simulating the MLD in Arctic regions, with large biases between the models and the observational data. In the present study, we aim to substantiate those discrepancies by assessing the skills of the ocean–sea ice GCM that participated in the Ocean Model Intercomparison Project (OMIP). We study the ability of these models to reproduce the seasonal cycle of the MLD in the ice-covered regions of the pan-Arctic seas. Specifically, we focus on the central Arctic Ocean, Beaufort Sea, Chukchi Sea, East Siberian Sea, Laptev Sea, Kara Sea and Barents Sea. In these regions, the MLD varies seasonally from 20 to 80 m in winter to 5 to 30 m in summer. Peralta-Ferriz and Woodgate (2015) showed that, in these areas, the MLD is strongly correlated to the ocean stratification and the wind mainly affects the ML during ice-free periods. Our goal here is to study the ability of OMIP models to reproduce the fall and winter deepening of the MLD compared to the Monthly Isopycnal Mixed layer Ocean Climatology (MIMOC) (Schmidtko et al., 2013) and Ice-Tethered Profilers (ITP) observations (Toole et al., 2011; Krishfield et al., 2008). We describe and quantify their biases, and we give some insights about the origin of the differences by using a simplified surface model inspired from the work of Martinson (1990). We focus on the fall and winter seasons because we aim to identify the origins of inter-model differences, which are much larger during these seasons.

The paper is organized as follows. Section 2 gives a brief description of the OMIP dataset, MIMOC climatology, and ITP observational data. Section 3 presents a diagnosis of the MLD in the central Arctic Ocean simulated by the OMIP models, and analyzes other variables relevant to understand ML seasonal changes such as the sea-ice concentration, the surface fluxes, the salinity profiles, and the ocean stratification. We also describe the simplified surface model and assess its skills with respect to the OMIP models in the central Arctic as well as in the other pan-Arctic seas. Finally, Section 4 presents concluding remarks and discusses implications of our work.

On the ability of OMIP models to simulate the ocean mixed layer depth and its seasonal cycle in the Arctic Ocean

2. Method

In this section, we briefly present the selected OMIP models and the observational data. MIMOC provides us with monthly observational data of the MLD (Schmidtko et al., 2013). MIMOC climatology is available at the National Oceanic and Atmospheric Administration, and it contains fields of ocean physical properties such as density, temperature, and salinity as a function of depth. Such values are obtained by conductivity - temperature - depth (CTD) instruments from shipboard data of the World Ocean Database, Ice-Tethered Profilers (ITP) and Argo Program. Due to data availability, the climatology is set-up between 2007 and 2011. MIMOC has a spatial resolution of 0.5° from 80° S to 90° N, and vertical resolution of 81 levels. The MLD is calculated using the algorithm of Holte and Talley (2009), which performs a statistical optimization based on traditional threshold and gradient methods over temperature, salinity and density individual profiles, thereby improving the accuracy of the depth between homogeneous mixed layer and turbulent mixing. As previously discussed by Schmidtko et al. (2013), this methodology yields a good agreement with the common threshold density criteria $\Delta \rho = \rho(z) - \rho(z_{ref}) = 0.03\,Kg/m^3$ used in the OMIP framework – also known as the *sigma-t* criterion (Griffies et al., 2016). This criterion has been introduced by Levitus (1982) and defines the MLD as the position from the shallowest depth down to the first depth for which the relative difference of density exceeds $0.03\,Kg/m^3$. Note that the surface level is only indicative. In the model simulations, it is defined in an *ad-hoc* manner and could vary from one model to another (Treguier et al., 2023). In order to estimate the impact of averaging different datasets and observations in MIMOC, we also computed directly the MLD from individual Ice-Tethered Profilers (ITP) (Toole et al., 2011; Krishfield et al., 2008), using the completed missions available at Woods Hole Oceanographic Institution (WHOI). We calculate the vertical potential density profiles using the TEOS-10/GSW (Gibbs Sea Water) Python library from the conservative temperature and the absolute salinity profiles. We applied the *sigma-t* criterion to compare ITP observational data with OMIP models, where the reference surface depth for ITP is more or less 5 meters. The ITP includes data from 2004 until 2019, with the majority of the observations between the years 2007 to 2015. We use here the ITP data from 2004 until 2011. Finally, we use the OSI-450 observational dataset for sea ice concentration (Lavergne et al., 2019). The OSI-450 dataset is available at the EUMETSAT data services, and it contains the sea ice concentration calculated from swath observations. The period covered by OSI-450 observational data goes from January 1979 to December 2015, and its grid spacing is about 25 Km. We have used the mean over the period covered by MIMOC data for consistency (2007-2011).

For the GCM models, we use models participating in the OMIP project. We work with models that contributed to both phases of the project: OMIP-I using as forcing the Coordinated Ocean-ice Reference Experiments version 2 (Griffies et al., 2016, CORE-II) and OMIP-II using as forcing the updated Japanese 55-year atmospheric reanalysis (Tsujino et al., 2020, JRA55-do). In order to compare models with observational data, we set-up two climatologies: between 2007 and 2009 for OMIP-I and between 2007 and 2011 for OMIP-II, both using the last cycle (sixth) of the protocol. The difference between the two periods is due to OMIP-I experiments ending in 2009. Our results and conclusions are not affected by this set-up. Our study uses the variables:

- ocean mixed layer depth (*mlotst*), for which the models follow the previously explained *sigma-t* criterion;

- sea ice mass change from thermodynamics (*sidmassth*), defined as the ice mass balance due to surface and basal heat fluxes, *i.e.* melting, sublimation and freezing;

- sea water salinity (*so*), defined as the salt content of sea water (it is a dimensionless variable expressed in parts per thousand);

- sea water potential temperature (*thetao*), defined as the mean potential temperature in °C using as reference the ocean surface;

- sea ice concentration (*sicon*), defined as the percentage of the grid cell covered by sea ice.

The definitions of these variables follow the OMIP protocol (Griffies et al., 2016). OMIP models do not generically produce the *sidmassth* variable, hence we restrict our analysis to those which do. We thus work with a subsample of 10 models with different ocean and sea ice components, as well as vertical resolution, and for which the nominal resolution ranges between 1° and 0.25° (see Table. 1). It is worth mentioning that all variables are interpolated to the MIMOC nominal spatial resolution before analyzing them.

On the ability of OMIP models to simulate the ocean mixed layer depth and its seasonal cycle in the Arctic Ocean
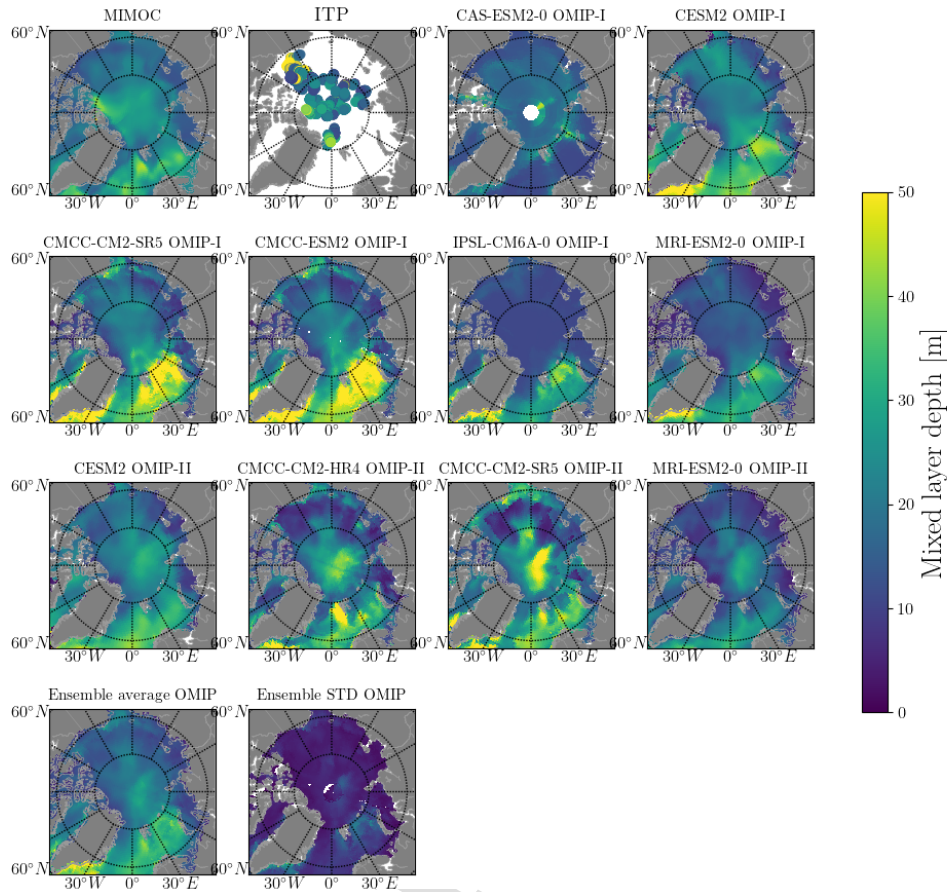

Figure 1: MLD maps in September for the MIMOC climatology, the ITP observational data, each OMIP model, the ensemble average of the models, and the ensemble standard deviation. Data is averaged in time between 2007-2009 for OMIP-I and between 2007-2011 for OMIP-II. ITP data correspond to the individual profiles from 2007 until 2011. A brief description of the OMIP models is shown in Table 1.

3. Results

3.1. Mixed layer in permanent ice-covered regions

Our analysis focuses first on the central Arctic Ocean, geographically defined here as the region from 80° N to the North pole. We first single out this area because it contains the largest sea ice extent in the Arctic region and is likely the region where vertical mass exchanges between sea ice and the MLD are most dominant, in addition to the wind-driven mixing in the upper part of the ocean and horizontal advection exchanges that potentially play a major role in all regions. Fig. 1 and Fig. 2 show the pan-Arctic MLD spatial distributions from MIMOC, ITP profiles, and OMIP models with the ensemble average of the models and its standard deviation in September and March, respectively. In

On the ability of OMIP models to simulate the ocean mixed layer depth and its seasonal cycle in the Arctic Ocean
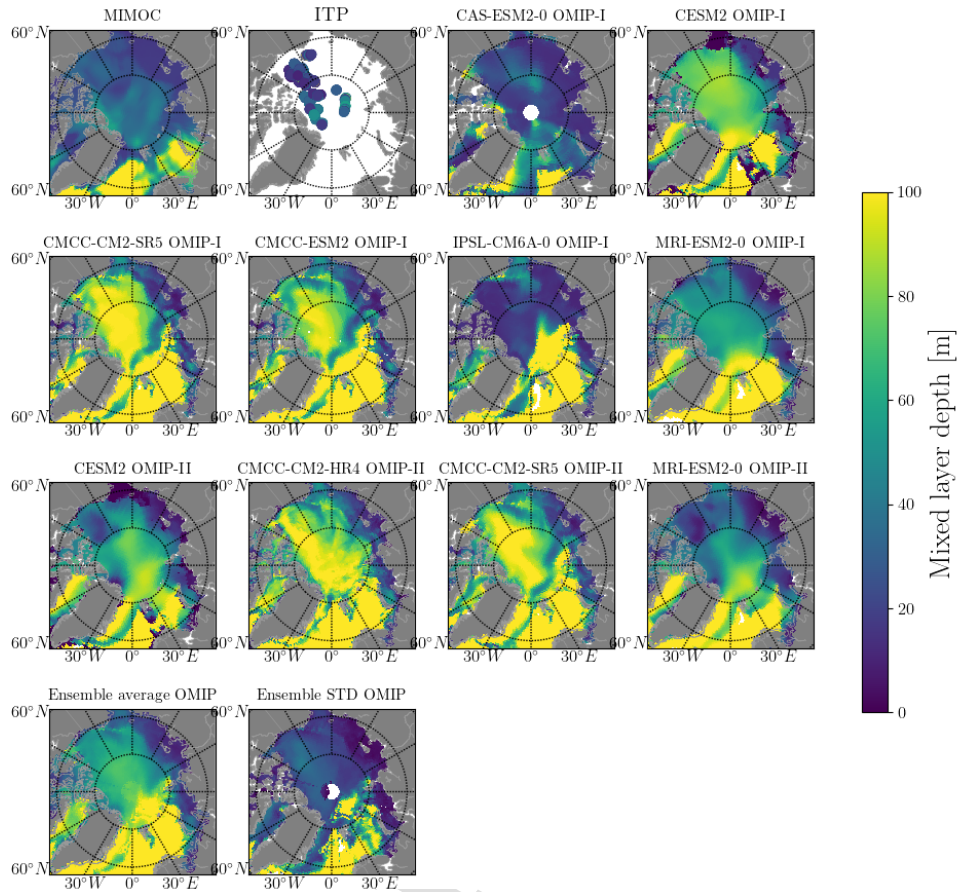

Figure 2: MLD maps in March for the MIMOC climatology, the ITP observational data, each OMIP model, the ensemble average of the models, and the ensemble standard deviation. Data is averaged in time between 2007-2009 for OMIP-I and between 2007-2011 for OMIP-II. ITP data correspond to the individual profiles from 2007 until 2011. A brief description of the OMIP models is shown in Table 1.

September, MIMOC and OMIP models have a shallow and quite homogeneous mixed layer. The OMIP MLD ensemble average has a similar behavior to individual models, and the ensemble standard deviation reaches only a few meters. The ITP profiles display larger spatial variability with some deeper spots compared to MIMOC and OMIP models. The disagreement between models and observations is higher in March. Many models tend to systematically overestimate the MLD by several tens of meters compared to the MIMOC and the ITP observational data. The ensemble average also displays deeper ML compare to observational data, with a large standard deviation in the central Arctic Ocean North of Svalbard and in the Barents Sea. CORE-II-forced models studied by Ilıcak et al. (2016) display a similar behavior with strong biases of the March MLD compared with the MIMOC dataset.

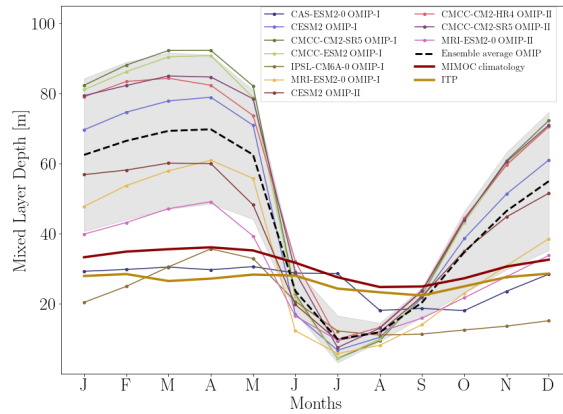On the ability of OMIP models to simulate the ocean mixed layer depth and its seasonal cycle in the Arctic Ocean

Figure 3: Seasonal cycle of the MLD in the central Arctic Ocean. Data is averaged in time between 2007-2009 for OMIP-I and between 2007-2011 for OMIP-II and ITP. Data is averaged in space between 80° N to 90° N in latitude and 180° W to 180° E in longitude. Solid lines with points represent OMIP models, the black dashed-line is the ensemble average of those models, the black-shading range is the ensemble standard deviation, and the blue dashed-line is the average of observational data. Red and yellow solid lines represent the MIMOC climatology and the ITP profiles, respectively.

145　　We now analyze the seasonal cycle of the spatially averaged MLD. This cycle is shown in Fig. 3 for all OMIP
146　models, MIMOC climatology and ITP observations. We observe that the ML from MIMOC and ITP observational data
147　remains shallow during the whole year. Both seasonal cycles exhibit less than 10 meters of amplitude, only varying
148　between 25 meters at the low summer value and 35 meters at the peak winter value for MIMOC, and between 22 and
149　28 meters for ITP observations. Please note that the seasonal cycle from ITP observational data displays a different
150　behavior than in Peralta-Ferriz and Woodgate (2015), where they show a larger amplitude of the MLD seasonal cycle
151　in the central Arctic Ocean. The differences in the MLD criterion explain it: In Peralta-Ferriz and Woodgate (2015),
152　they calculate the MLD using the threshold criterion $\Delta\rho = 0.1\,Kg/m^3$. In contrast, in our study, we use the *sigma-t*
153　criterion $\Delta\rho = 0.03\,Kg/m^3$. Several criteria are used to compute the MLD in the Arctic region (Cole and Stadler,
154　2019; Stranne et al., 2018; Polyakov et al., 2013; Timmermans et al., 2012; Mizobata and Shimada, 2012; Jackson
155　et al., 2012), and there is still no clear consensus as to which criterion is the best. However, our aim here is to compare
156　OMIP models and then we employ the threshold $0.03\,Kg/m^3$ criterion to obtain the MLD. It explains our choice of
157　criterion.
158　　Additionally, Fig. 3 shows that most OMIP models exhibit a large dispersion compared with the observational data
159　(MIMOC and ITP). All the models display two clear seasonal phases: (i) In spring, almost all the modeled ML are
160　deeper than the observational data, and in summer all the models underestimate it by about 15 meters. (ii) In fall and
161　winter, the simulated ML becomes deeper, and discrepancies with observations reach up to several tens of meters in
162　some models. The differences are also large between the models. The standard deviation of the OMIP models ensemble
163　average reaches about 20 meters. For instance, CMCC models generate too-deep mixed layers, and the CAS-ESM2-0
164　model a too-shallow MLD. Comparing OMIP-I to OMIP-II protocols, a systematic decrease exists for the amplitude
165　of the MLD seasonal cycle in the latter case. This effect was previously observed by Tsujino et al. (2020), presumably
166　due to the more significant freshwater discharge from Greenland in the OMIP-II models. For CMCC-CM2-SR5, this
167　trend is hardly significant and may as well be due to statistical biases. In such cases, one could not rule out that OMIP-II
168　protocols may produce larger MLD at a very local level, as for instance reported by Shu et al. (2022) comparing the
169　ensemble average spatial distribution of OMIP-I and OMIP-II in the central Arctic Ocean. For CESM2 and MRI-ESM2-
170　0, the difference is clearly visible, with differences in the March MLD of 17 and 11 meters, respectively. However, even
171　in this case, switching from OMIP-I to OMIP-II hardly compensates the biases with the observed MLD. Additionally,

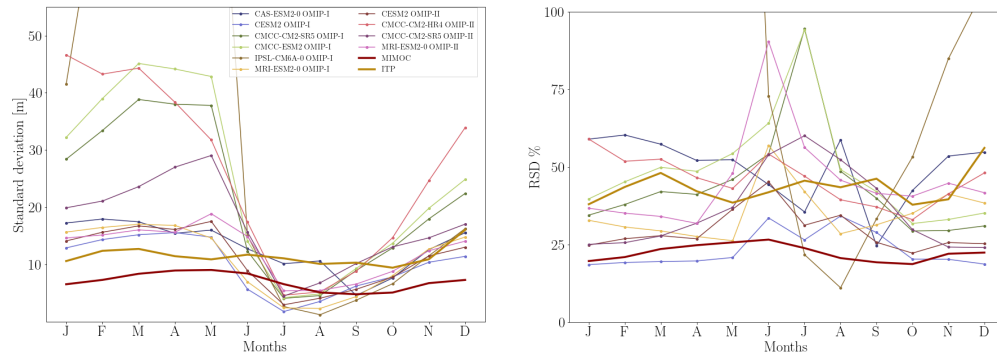On the ability of OMIP models to simulate the ocean mixed layer depth and its seasonal cycle in the Arctic Ocean

Figure 4: Left panel: Spatial standard deviation of OMIP models, MIMOC climatology and ITP observational data, in the central Arctic Ocean. Right panel: Spatial relative standard deviation (RSD) of OMIP models, MIMOC climatology and ITP observational data, in the central Arctic Ocean. The RSD is defined as the percentage of the ratio between the standard deviation and the mean value. Data is averaged in in space between 80° N to 90° N in latitude and 180° W to 180° E in longitude.

increasing the resolution does not seem to correct the biases either: The model with the highest resolution is CMCC-CM2-HR4 OMIP-II, and it simulates close to the exact same cycle as its low-resolution counterpart CMCC-CM2-SR5 OMIP-II.

To quantify the MLD spatial variability from OMIP models and observational data, we show their spatial standard deviation for each month in the left panel of Fig. 4. This quantity measures the dispersion of the MLD around the central Arctic Ocean. For most OMIP models and MIMOC dataset, the standard deviation remains lower than 10 meters over the entire year, while the standard deviation for ITP observational is slightly higher with values between 10 and 15 meters. The CMCC and IPSL models display a more significant standard deviation during fall and winter, where the IPSL model reaches more than 100 meters in March, April, and May. The right panel of Fig. 4 shows the relative standard deviation (RSD), defined as the percentage of the ratio between the standard deviation and the mean value. During the year, most OMIP models display a RSD smaller than 50%. It means that the spatial variability is not too large. However, CMCC-CM2-HR4 OMIP-II and CESM2 OMIP-II models reach large RSD of more or less 100%, and the IPSL-CM6A-0 OMIP-I model even has values close to 400%. These models have an important spatial variability, with standard deviation values larger than their mean. It is also observed in Fig. 2, where these models show important spatial differences in this region. Some studies distinguish between Eurasian and Makarov basins to have more homogenous conditions in the central Arctic Ocean (see, for instance, Peralta-Ferriz and Woodgate (2015)). We do not make this choice because the spatial variations are not too large in most OMIP models and MIMOC observational data.

3.2. Sea ice and ocean physical properties

Sea ice concentration. A key feature of the central Arctic Ocean is the presence of sea ice during the whole year. We refer to this area as a permanent ice-covered regions. The left panel of Fig. 5 illustrates the seasonal cycle of sea ice concentration at the surface of the ocean. A 100 % value means that the surface is fully covered by sea ice, while a lower value means that there exist uncovered sectors. Observational data shows that sea ice concentration in the central Arctic is approximately 100 % during fall, winter and spring, only decreasing to 80 % in summer, hence exhibiting a variation of about 20 % in magnitude. At a qualitative level, this decrease is correctly reproduced by most of the models. At a quantitative level, the OMIP-II models perform slightly better than their OMIP-I counterparts. In the former models, the sea ice concentration typically varies between 15 and 40 % from summer to winter. This is more faithful than the variation of 60 % simulated by CAS-ESM-0, CESM2, CMCC-CM2-SR5 and CMCC-ESM2 part of the OMIP-I experiment. This effect was previously noticed by Tsujino et al. (2020) and thoroughly explained by Lin et al. (2022) due to the change of shortwave radiation fluxes from OMIP-I to OMIP-II simulations.

On the ability of OMIP models to simulate the ocean mixed layer depth and its seasonal cycle in the Arctic Ocean
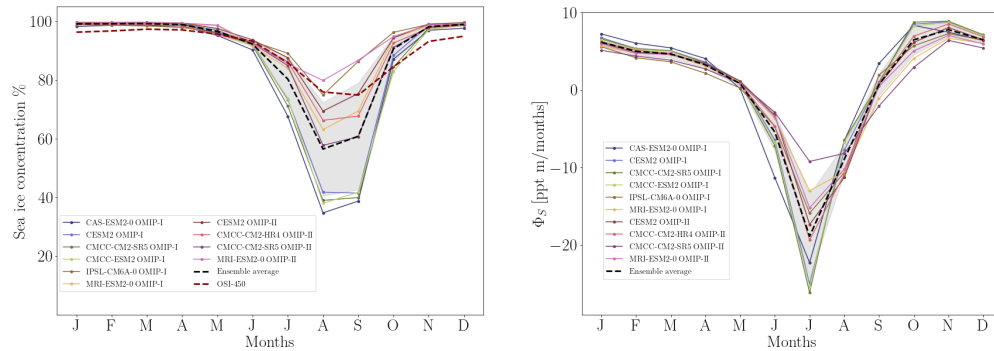

Figure 5: Left: Sea ice concentration seasonal cycle in the central Arctic Ocean. Color lines represent OMIP models sea ice concentration from *sicon* variable. The red dashed-line corresponds to the observational data OSI-45. Right: Seasonal cycle of the salinity flux in the central Arctic Ocean. Color lines represent OMIP models, and the salinity flux is derived from *sidmassth* variable. The black dashed-lines represent the ensemble average of OMIP models, and the black-shading ranges the ensemble standard deviation. Data is averaged in time between 2007-2009 for OMIP-I and between 2007-2011 for OMIP-II and OSI-45. Data is averaged in space between 80° N to 90° N in latitude and 180° W to 180° E in longitude.

Salt transfer. From a physical point of view, the permanent presence of a sea ice layer reduces the interactions between the upper ocean and the atmosphere, for instance limiting the shear produced by winds and waves. The ML characteristics are then largely determined by the interactions between the ML and the sea ice. The rough physical picture is then the following: In fall and winter, the growth of sea ice is associated with brine rejection, *i.e.* salt is rejected from crystal structures of water ice, increasing salinity in the upper layer of the ocean. In spring and summer, sea ice melts and freshwater goes to the ocean, decreasing the salt concentration. The details of the mass transfer may depend on the dynamics of each model and its parameterization. For instance, Barthélemy et al. (2015) studied the impact of this process in the ocean using the NEMO-LIM3 global ocean–sea ice model. We can estimate this transfer of mass, associated with sea ice formation and melting, directly from the *sidmassth* output in the OMIP protocol. We convert it into an equivalent salt flux, measured as the meters of salt transferred in each month. The right panel of Fig. 5 shows the seasonal cycle of the corresponding salt flux Φ_S for OMIP models. During fall and winter, when the salt flux is positive, inter-model comparison displays small variations: for instance the mean value in January is 6.13 [ppt meters/month] with a standard deviation of 0.6 [ppt meters/month]. Fig. A.1 shown in Appendix reveals that all the models simulates a similar amount for salt transfers towards the ocean totaled over the winter months, without any clear link with the MLD in winter. This suggests that the biases observed in the OMIP MLD are not due to discrepancies related to the sea ice mass budget but rather to other processes involved in the MLD seasonal evolution, such as wind-driven and horizontal exchanges.

Vertical salinity profile and stratification. The fluxes from sea ice affect the physical properties of the ocean, in particular the vertical density profile. This in turn causes variations in the ocean stratification. We recall that the MLD in OMIP models is determined by applying a density criterion, which is by construction sensitive upon the underlying vertical density profile. While ocean density is in general a non-linear function of temperature and salinity, the density in permanent ice-covered regions is mostly controlled by ocean salinity and temperature variations are relatively small in the top layers of the ocean. – see for instance Gettelman and Rood (2016, Chapter 6). This behavior is indeed observed in OMIP models, when monitoring the spatially averaged ocean salinity and temperature vertical profiles (hereafter simply referred to as the "mean salinity profile" and "mean temperature profile"). Fig. 6 shows that in most of the OMIP models and in the MIMOC dataset, while the temperature is not vertically changing much (less than 1° C), the first abrupt change of the mean salinity profile indicates the bottom of the mixed layer and the beginning of the halocline. This suggests that in ice-covered regions, including but not limited to the central Arctic, the halocline shape provides a reliable indicator to estimate the ocean stratification.

On the ability of OMIP models to simulate the ocean mixed layer depth and its seasonal cycle in the Arctic Ocean
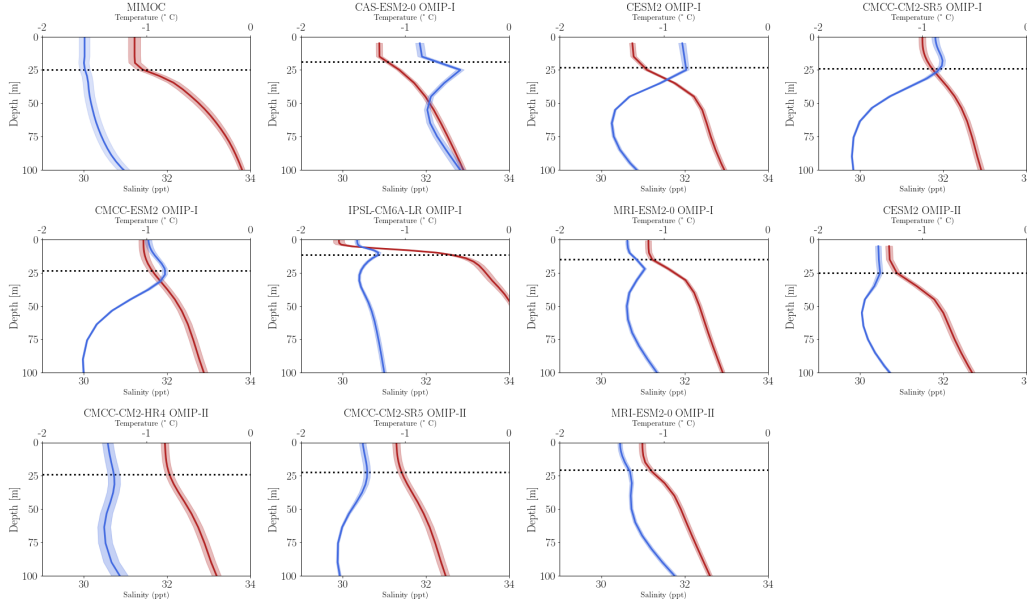

Figure 6: Vertical salinity (red lines) and temperature (blue lines) profiles of September for OMIP models and MIMOC climatology. The shading ranges correspond to the spatial standard deviation, and the dotted lines show the MLD. The OMIP dataset is averaged in space between 80° N to 90° N in latitude and 180° W to 180° E in longitude.

The vertical stratification below the mixed layer at the month m is estimated here as the mean vertical gradient of the mean salinity profile S_m between the MLD h_m and the current depth z, that is

$$\gamma_m(z) = \frac{S_m(z) - S_m(h_m)}{z - h_m}. \tag{1}$$

The vertical salinity profile is not linear, as shown in Fig. 6, hence the stratification varies with depth. The vertical salinity profile also varies with time. To monitor its evolution, we compute the ocean stratification of the current month m using Eq. 1 (see Fig. 7). Please note that the stratification is calculated over the halocline profile, using as an approximation for z the depth corresponding to the ML of the following month. As expected, all OMIP models and MIMOC climatology display a decrease in ocean stratification as winter progresses, as a consequence of the transfer of salt from sea ice. Among the OMIP models, the largest variations between models for the stratification occur in September and decreases over fall and winter. The fall/winter evolution of OMIP models ocean stratification is far more pronounced than MIMOC observational data. Focusing on September, we note that OMIP models with ocean stratification values closer to MIMOC also show a seasonal cycle similar to observational data.

3.3. A surface model for the salt balance

Surface model. We propose to use a simple framework to reproduces the fall and winter deepening of the ML, in terms of the salt balance and mixed layer dynamics. This framework is inspired by the work of Martinson (1990) and is illustrated in Fig. 8. The model neglects the non-linearity of the vertical salinity profile, as well as the effect of the wind stress and horizontal exchanges. It links the salt flux Φ_S flowing into the ocean between September and month m as

$$\Phi_S(m) = \left(S_{m+1}(h_{m+1}) - S_m(h_m)\right) \frac{h_{m+1} + h_m}{2}, \tag{2}$$

On the ability of OMIP models to simulate the ocean mixed layer depth and its seasonal cycle in the Arctic Ocean
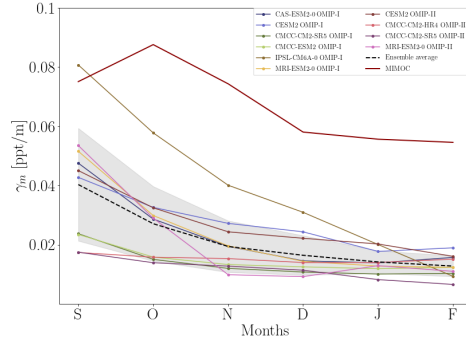

Figure 7: Ocean stratification calculated from Eq. 1 between the base of the ML and the depth corresponding to the ML of the following month for OMIP models and MIMOC climatology. The x-axis corresponds to the months of September, October, November, December, January, and February. The black dashed-line represents the ensemble average of OMIP models, and the black-shading range is the ensemble standard deviation.

where h_m and h_{m+1} represent the MLD at month m and $m + 1$, and $S_m(h_m)$ and $S_{m+1}(h_{m+1})$ the salinity values at the corresponding MLD. In principle, the salt flux, the MLD, and the salinity depend on the latitude and longitude coordinates. For the sake of clarity, we later omit to explicitly feature this spatial dependence. Eq. (2) can be interpreted as a midpoint approximation, as illustrated in the right panel of Fig. 8. It relies on the observation that essentially, in the OMIP models, the vertical salinity profiles stay piecewise linear during fall and winter months, as shown in the left panel of Fig. 8. To estimate the salinity at the MLD, we use the data-driven approximation

$$S_{m+1}(h_{m+1}) \simeq S_m(h_m) + \gamma_{Sept}(h_{Mar}) \left(h_{m+1} - h_m \right),\tag{3}$$

involving the September stratification until the MLD in March $\gamma_{Sept}(h_{Mar})$, which is obtained by Eq. (1). Using Eq. 3, the salt flux of Eq. (2) becomes

$$\Phi_S(m) = \frac{\gamma_{Sept}(h_{Mar})}{2} \left(h_{m+1}^2 - h_m^2 \right).\tag{4}$$

From this formula, one can now explicitly relate the MLD at month m to the MLD at month $m + 1$ as

$$h_{m+1} = h_m \sqrt{1 + \frac{2\Phi_S(m)}{h_m^2 \gamma_{Sept}(h_{Mar})}}.\tag{5}$$

We use Eq. 5 to reproduce the fall and winter ML deepening for each OMIP model. The formula depends on two main inputs, namely the salt flux $\phi_S(m)$ and the September stratification between the basis of the ML and a depth corresponding to the ML in March $\gamma_{Mar}(h_{Mar})$. To prescribe those values, we use the outputs of the OMIP models. Values for the salt flux ϕ_S correspond to the ones previously shown in the right panel of Fig. 5. The September stratifications for the various models are calculated from the OMIP salinity profiles. We later discuss two series of simulations obtained either with

(i) a local methodology, in which Eq. 5 is applied at each grid point (x, y) using the local value for the September stratification $\gamma_{Sept}(h_{Mar})$ and salt fluxes $\Phi_S(m)$ – The local MLD $h_{m+1}(x, y)$ obtained from the surface model is then averaged in space for the plots;

(ii) an average methodology, in which Eq. 5 is applied to the salinity gradients and salt fluxes averaged in space;

The first methodology should in principle be able to capture spatial fluctuations, but may be more sensitive to the horizontal transport that is neglected in the present framework. In contrast to the second one, which is only driven by averaged OMIP output quantities.
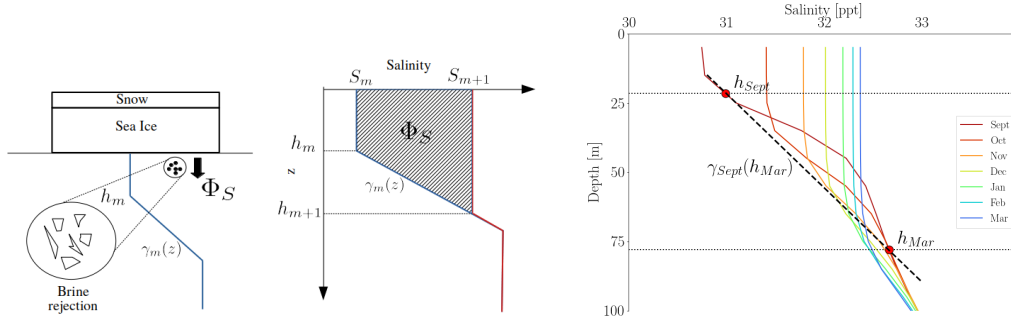
Figure 8: Left panel: Illustration of the salt balance dynamics prescribed by Eq.(5). Left: brine rejection mechanism. Right: piecewise modeling of the ML, where Φ_S represents the salt flux, $\gamma_m(z)$ the ocean stratification, h_{m+1} the MLD of the month $m + 1$, h_m the MLD of the month m, S_{m+1} the vertical salinity profile of the month $m + 1$, and S_m the vertical salinity profile of the month m. Right panel: Month-to-month evolution of the first 100m of the vertical salinity profile for the CESM2 OMIP-I model between September and March. Dotted lines represent the MLD in September and March. Dashed line represents the ocean stratification $\gamma_{Sept}(h_{Mar})$, with h_{Mar} is the MLD in March.

Surface model vs OMIP models We here analyze the skills of both methodologies to reproduce the fall and winter ML deepening. Fig. 9 displays the full fall and winter MLD seasonal cycle simulated by the surface model for each OMIP model and MIMOC observational data. The fall and winter deepening from MIMOC observational data is only shown in the average methodology because we do not have access to salt flux observations. We use as an approximation the ensemble average salt flux from OMIP models. At a qualitative level, the surface model provides a correct representation of the MLD growth in the first three months (October, November and December) for both methodologies, but the local one displays remarkable quantitative agreement with most of the OMIP seasonal cycles. We relate this feature to the fact that averaged inputs loose tracks of the spatial fluctuations, which are present in OMIP simulations. Specifically, we observe strong spatial variations in the ocean stratification, measured here by using the salinity profile (see Fig.A.2 and Fig.A.3 in Appendix). Besides, we notice that the models CAS-ESM2-0 OMIP-I and IPSL-CM6A-0 OMIP-I have most disagreement with the surface model. To quantify this behavior, we have calculated the MLD relative error

$$\text{relative error} = \frac{MLD_{OMIP/MIMOC} - MLD_{Surface}}{MLD_{OMIP/MIMOC}}, \tag{6}$$

where $MLD_{OMIP/MIMOC}$ corresponds to the MLD from OMIP models or MIMOC observational data and $MLD_{Surface}$ is the estimated MLD from the surface model. The March MLD error is shown in the bottom right panel of Fig. 9. Almost all OMIP models display less than 15 % error, and MIMOC more or less 25 % of error.

Among the OMIP models whose MLD in March is quasi perfectly reproduced by the simple model, we find the models CESM2 OMIP-I and CMCC OMIP-I. For those two models, the surface model displays less of 10 % error. We however recall that, compared to observational data, both CESM2 OMIP-I and CMCC OMIP-I largely overestimate the amplitude of MLD seasonal cycle and, in particular, the MLD in March. The fact that a simplified model, which only considers the vertical salt flux, captures much of the MLD evolution when those values are biased compared with observational data, suggests that the MLD modeling could improve by including other processes responsible for changes in MLD, such as wind-driven and horizontal exchanges, neglected in the simple model. Conversely, CAS-ESM2-0 OMIP-I and IPSL-CM6A-0 OMIP-I display the largest mismatch with the surface model, while those models are the OMIP models which most consistently reproduce the MLD seasonal cycle in comparison to observational data. This suggests that those models represent better the ML dynamics and that this dynamics is more complex that the one of the simple surface model.

We conclude this section by noticing that there exists a strong relationship between the September ocean stratification and the March MLD in OMIP models. This relationship is shown in the left panel of Fig. 10, where we

On the ability of OMIP models to simulate the ocean mixed layer depth and its seasonal cycle in the Arctic Ocean
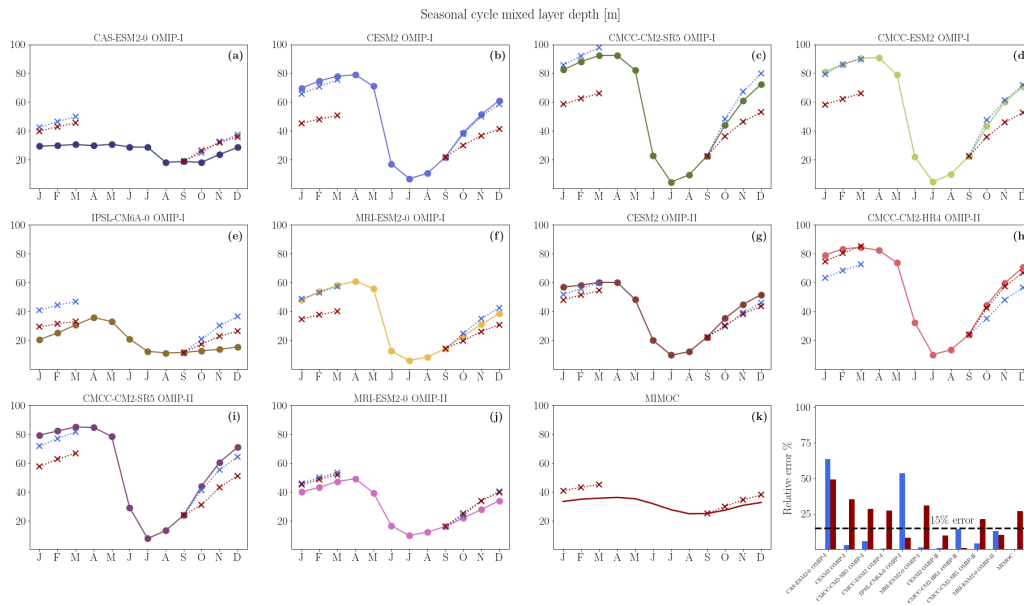
Seasonal cycle mixed layer depth [m]

Figure 9: Reproduction of the seasonal cycle of the MLD from each OMIP model and MIMOC observational data in the central Arctic Ocean using Eq. 5. Blue dashed line use the values in each grid point. Red dashed line use the averaged values of the salinity gradient and the salinity flux. Please note that while the seasonal cycle is here represented with months varying from January to December, our iteration procedure uses September as initial time. Right bottom panel represents the relative March MLD error for each OMIP model, with the corresponding methodologies in red and blue color bars.

observe that deep mixed layers relate to weakly stratified oceans, while shallow mixed layers relate to strongly stratified oceans, as expected. Furthermore, compared to MIMOC dataset, the OMIP models with the best representation of the stratification in September are also the ones with the best mixed layer in winter. This suggests that the representation of the stratification is a strong signature of the MLD biases in OMIP models.

3.4. Adjacent seas of the central Arctic Ocean

We now analyze if a similar behavior for the MLD dynamics is present in neighboring seas of the central Arctic Ocean. Specifically, we look into the Beaufort, Chukchi, East Siberian, Laptev, Kara, and Barents Seas; their boundaries are shown in the right panel of Fig. 10. Their MLD seasonal cycle from MIMOC, ITP and OMIP models are displayed in Fig. 11. ITP observations are only available during the whole year for the Beaufort and Chukchi Seas, in the other regions, we only compare with MIMOC climatology. The seasonal cycle of the MIMOC MLD in the Beaufort, Chukchi, East Siberian, Laptev, and Kara Seas exhibits a similar behavior than in the central Arctic Ocean, characterized by a small seasonal amplitude and a shallow ML throughout the year – about 20 meters over the year. The behavior is quite different in the Barents Sea, where the MIMOC MLD seasonal cycle shows a high seasonal amplitude: It is characterized by a 60-meter difference between January and August, with a maximum MLD of 80 meters in January. In each region, the OMIP models differ strongly with each other, some having MLD close to the MIMOC one, while others overestimate it in winter by tens of meters. Regarding ITP observations, the MLD seasonal cycles in the Beaufort and Chukchi Seas are a few meters shallower compared to MIMOC, as already noticed for the central Arctic Ocean. The magnitude of the inter-model variations differs depending on the sea under consideration. In the Beaufort, Chukchi, Kara, East Siberian and Laptev Seas, discrepancies between models reach up to 30 meters on average. In the Barents Sea, the MLD inter-model variations reach more than 100 meters.

On the ability of OMIP models to simulate the ocean mixed layer depth and its seasonal cycle in the Arctic Ocean
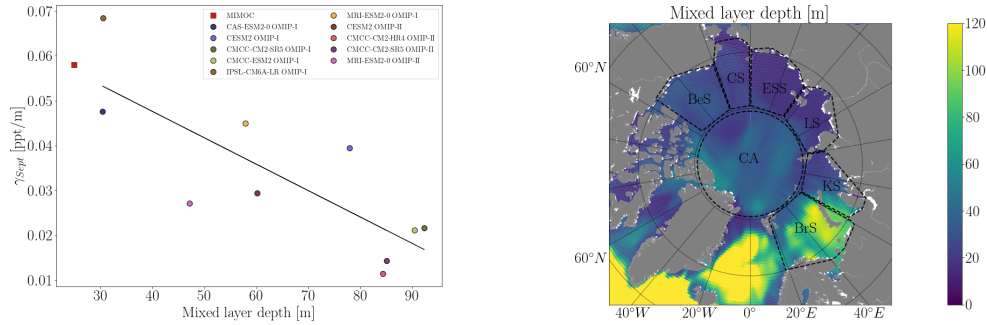

Figure 10: Left panel: Relation between the MLD in March and the ocean stratification in September until the MLD in March, for all OMIP models and MIMOC climatology. Right panel: Pan-Arctic MIMOC MLD map in March. The dashed lines show the boudaries of Beaufort (BeS), Chukchi (CS), East Siberian (ESS), Laptev (LS), Kara (KS), and Barents (BrS) Seas.
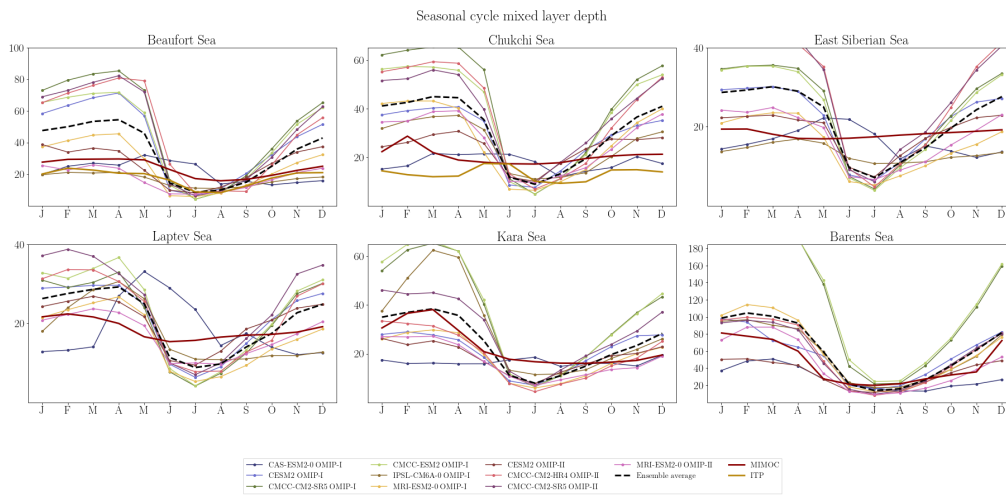

Figure 11: Seasonal cycle of the MLD in the Beaufort, Chukchi, East Siberian, Laptev, Kara and Barents Seas. Data is averaged in time between 2007-2009 for OMIP-I and between 2007-2011 for OMIP-II and ITP. Data is averaged in space between 80° N to 90° N in latitude and 180° W to 180° E in longitude. Solid colors represent OMIP models, black dashed-line the ensemble average of those models, and red dashed-line MIMOC climatology.

With the exception of the Barents Sea, the Arctic adjacent seas have more than 80% of sea ice concentration during winter months (see Fig.A.5 in Appendix). This suggests that, in these almost fully ice-covered regions, brine rejection has a large impact on the ML fall and winter dynamics, in addition to other processes such as wind-driven mixing and horizontal advection, similarly to the central Arctic Ocean. In these regions, the fall and winter salt flux shows small variations between models (see Fig. A.4 in Appendix).

To get more quantitative insights, we also applied the surface model in its averaged version for all OMIP models in each region. The relative errors of the March MLD are shown in Fig. 12. In the Beaufort and Chukchi Seas, the surface

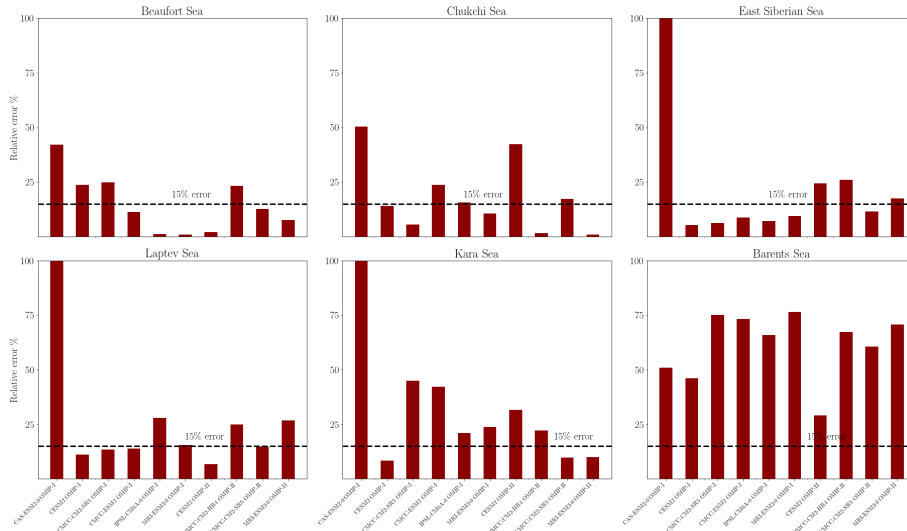On the ability of OMIP models to simulate the ocean mixed layer depth and its seasonal cycle in the Arctic Ocean

Figure 12: Relative error of the MLD seasonal cycle amplitude between OMIP outcomes and the MLD estimated using Eq. 5 with the averaged values.

model display a similar behavior than the central Arctic Ocean. Almost all OMIP models reach less than 15% error in the reproduction of the fall and winter MLD deepening. In the East Siberian and Laptev Seas, a more subtle feature is observed. The small relative errors are due to the shallow ML, and not to the good prediction of the surface model. In the Kara Sea, the relative errors are larger than in the other almost fully ice-covered regions, and then the surface model is not pertinent to explain the MLD variations. This could be due to the lower concentration of sea ice in winter compared to other regions, as well as exchanges with the Barents Sea. The surface model displays a poor ability to reproduce the fall and winter deepening of the ML in the Barents Sea. As expected, in this area, which is partly covered by sea ice (see Fig. A.5 in Appendix), the fall and winter ML deepening is not dominated by the salt balance associated with the exchanges with sea ice but is controlled by surface cooling, wind-driven mixing and horizontal advection. Those mechanisms are not considered by the surface model, explaining its poor performance at reproducing the results of the GCM models. Those results suggest that only the Beaufort and Chukchi Seas display similar behavior compared to the central Arctic Ocean: OMIP models with larger biases compared with observational data are the ones with the best representation using the simplest model, suggesting that this missing the impact of more complex processes leads to overestimating the MLD seasonal cycle.

As a side remark, large errors are obtained with the CAS-ESM2-0 OMIP-I model in some almost fully ice-covered regions. Fig. 11 shows that mismatches come from the model itself, with a poor representation of the MLD seasonal cycle in the East Siberian, Laptev and Kara Seas. This is confirmed by looking at its MLD spatial distribution during the whole year (see Fig. A.6 in Appendix). We observe that, during April, May and June, the CAS-ESM2-0 model simulates large MLD, especially on the East Siberian and Laptev coasts. Shu et al. (2022) suggest that one possible reason for these discrepancies is that the CAS-ESM2-0 model has the Canadian Arctic Archipelago passes closed.

Finally, in all the regions apart from the Kara Sea, OMIP models whose best ocean stratification compares the best to the MIMOC observational data also show the closest ML deepening at the end of the winter (see Fig. 13). Besides, only the Beaufort and Chukchi Seas display a strong relation between the stratification in September and the MLD at the end of winter, also observed in the central Arctic Ocean. This is compatible with the general idea that strongly stratified oceans lead to shallow ML, and weakly stratified oceans lead to deep ML. However, for the others regions, the relation is not so clear.

On the ability of OMIP models to simulate the ocean mixed layer depth and its seasonal cycle in the Arctic Ocean
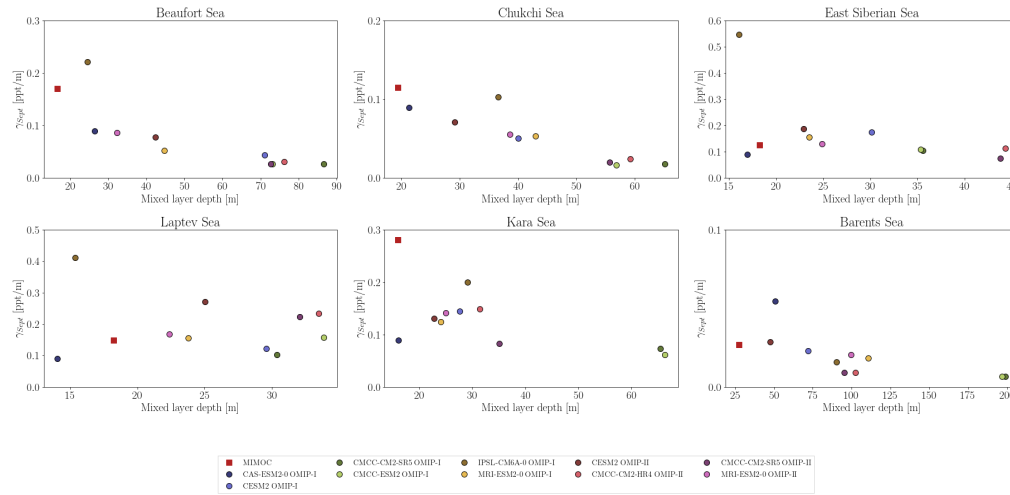

Figure 13: Relation between the mixed layer depth in March and the ocean stratification in September for the Beaufort (BeS), Chukchi (CS), East Siberian (ESS), Laptev (LS), Kara (KS), and Barents (BrS) Seas.

4. Discussion and conclusion

We have studied the ability of OMIP models to reproduce the fall and winter deepening of the ML in pan-Arctic seas: central Arctic Ocean, Beaufort, Chukchi, East Siberian, Laptev, Kara, and Barents Seas. We have shown that in all these regions, OMIP models poorly represent the MLD seasonal cycle. In summer, a large part of OMIP models underestimates the MLD by about 15 meters compared to MIMOC climatology. During fall and winter, large biases appear with some models with very deep ML and others with values closer to observational data. In particular, we have observed that the CAS-ESM2-0, IPSL-CM6A-0, and MRI-ESM2-0 models from OMIP-I protocol are consistent enough in simulating the fall and winter deepening in more than one region of the pan-Arctic seas. However, CMCC models at low and high resolution and from OMIP-I and OMIP-II protocols, display too depth ML in almost all the seas. During these seasons, discrepancies between models reach up to 30 meters on average in all the regions, except in the Barents Sea, where the MLD inter-model variations reach more than 100 meters. We showed that OMIP models provide consistent sea ice concentrations and ice-ocean salt fluxes. At the same time, discrepancies have been observed in the ocean stratification at the beginning of the sea ice growth season. In the central Arctic Ocean, Beaufort, and Chukchi Seas, we have shown a strong relationship between the ocean stratification in September and the MLD at the end of winter: Weakly stratified oceans lead to large MLD and strongly stratified oceans lead to small MLD. It should be noted that this is not a causal relation, and then we can also reverse the relationship. For instance, shallow ML in winter leads to strongly stratified oceans at the beginning of the fall. Furthermore, OMIP models with similar ocean stratification compared to MIMOC observational data perform better in the reproduction of the MLD at the end of the winter.

We use the MIMOC climatology and the ITP observational data to compare OMIP models. We have found that both observational data have similar MLD seasonal cycles in the central Arctic Ocean, Beaufort and Chukchi Seas, using the OMIP-recommended density threshold of $0.03\ Kg/m^3$ to compute the MLD. The depth of the mixed layer varies depending on the criterion used. For instance, the ML is deeper using a criterion of $0.1\ Kg/m^3$ instead of $0.03\ Kg/m^3$ in pan-Arctic regions (Peralta-Ferriz and Woodgate, 2015). The different choices of criterion by different authors make model-data comparisons more difficult. Additionally, due to ITP data availability, the East Siberian, Laptev, Kara, and Barents Seas Seas are only compared with MIMOC climatology. In principle, MIMOC climatology is strongly based on Argo/ITP observation during this period. The spatial distribution of Argo float data is very sparse in Laptev and Kara Seas (Fournier et al., 2020). It suggests that MIMOC may not represent the full reality regarding MLD in these regions.

On the ability of OMIP models to simulate the ocean mixed layer depth and its seasonal cycle in the Arctic Ocean

386 We were able to reproduce the fall and winter deepening of the ML simulated by the OMIP models using a simple
387 surface model based on the vertical salt balance dynamics. This model uses as inputs the vertical salinity gradient in
388 September and the salinity flux from OMIP models. In the central Arctic Ocean, Beaufort, and Chukchi Seas, we have
389 noted that OMIP models with the largest relative errors from the reproduction of the fall and winter ML deepening
390 using the surface model, are the ones that display more realistic values of the MLD seasonal cycle compared with
391 observational data. It suggests that these models accurately reproduce the ML dynamics and that these dynamics is
392 more complex that the one of the simple surface model. In the other regions, the MLD dynamics is different. For
393 instance, in the Barents Sea, the retreat of ice cover during summer is larger than in the central Arctic, hence favoring
394 exchanges with the atmosphere. This feature is likely to foster deeper ML: the Barents Sea displays a larger MLD
395 seasonal cycle than the other regions.

396 Still, and despite these different behaviors, the poor modeling of GCM in pan-Arctic seas seems to be linked to
397 a very simple modeling of the processes involved in its dynamics. Here, we focused on the vertical mass exchanges
398 associated with salt balance. A natural perspective is to study the impact of the other mechanisms, such as surface
399 cooling, wind-driven mixing, and horizontal advection. Furthermore, an appealing perspective to our work concerns
400 the study of the MLD inter-annual variability, particularly the effect of the feedback between the sea ice and the mixed
401 layer. In this prospect, we expect to analyze the GCM of the coupled part of the CMIP6 protocol from the historical
402 simulations, in the same line as previous works by Watts et al. (2021) and Keen et al. (2021) in the inter-model analysis
403 of sea-ice and mass budget in the Arctic.

CRediT authorship contribution statement

405 **S Allende:** Conceptualization of this study, Methodology, Formal analysis, Writing - Original Draft, Visualization
406 . **T Fichefet:** Conceptualization of this study, Writing - Review & Editing . **H Goosse:** Conceptualization of this
407 study,Writing - Review & Editing . **AM Treguier:** Conceptualization of this study, Writing - Review & Editing .

Declaration of competing interest

409 The authors declare that they have no known competing financial interests or personal relationships that could have
410 appeared to influence the work reported in this paper.

Acknowledgments

A. Appendix

416 We here compile additional figures related to: the relation between the MLD in March and the cumulative salt flux
417 (Fig. A.1); the sea surface salinity maps from the MIMOC dataset and OMIP models in September (Fig. A.2) and
418 March (Fig. A.3); the salinity flux in the pan-Arctic seas (Fig. A.4); the sea ice concentration in the pan-Arctic seas
419 (Fig. A.5); and the spatial distribution of the sea surface salinity from the CAS-ESM2-0 OMIP-I model (Fig.A.6).

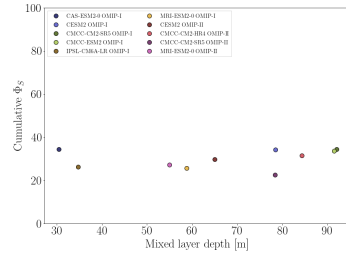On the ability of OMIP models to simulate the ocean mixed layer depth and its seasonal cycle in the Arctic Ocean

Figure A.1: Relation between the MLD in March and the cumulative salt flux (ppt m/months) during fall and winter in the central Arctic Ocean.
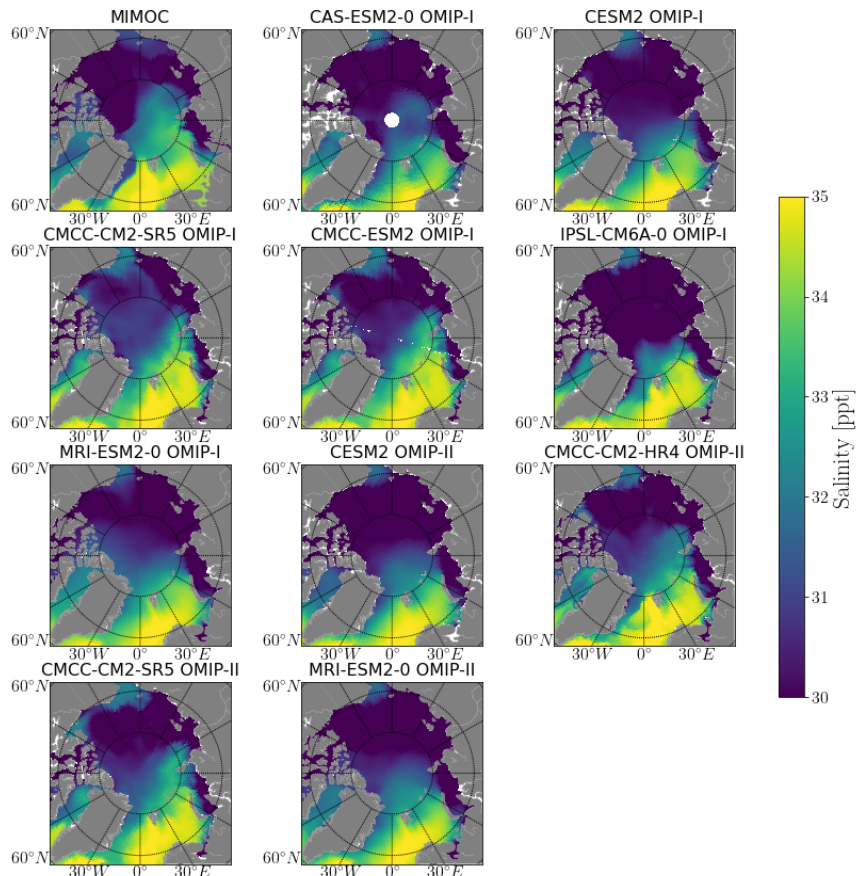

Figure A.2: Sea surface salinity (ppt) maps in September from the MIMOC climatology (top left) and the OMIP models listed in Table 1.

On the ability of OMIP models to simulate the ocean mixed layer depth and its seasonal cycle in the Arctic Ocean
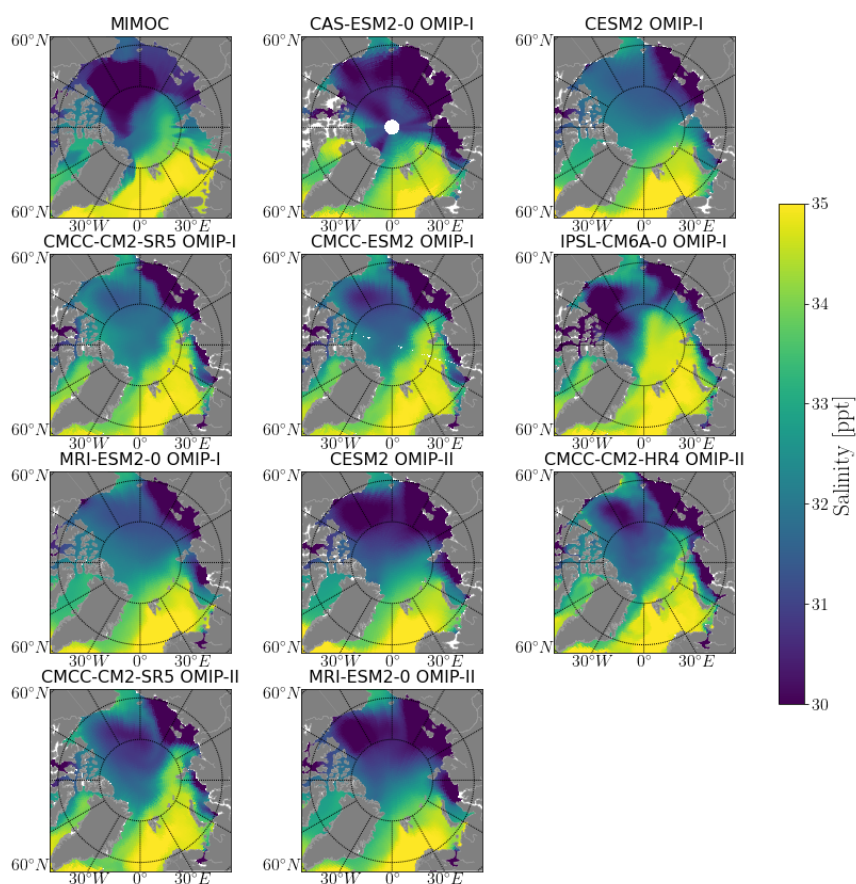

Figure A.3: Sea surface salinity (ppt) maps in March from the MIMOC climatology (top left) and the OMIP models listed in Table 1.

On the ability of OMIP models to simulate the ocean mixed layer depth and its seasonal cycle in the Arctic Ocean
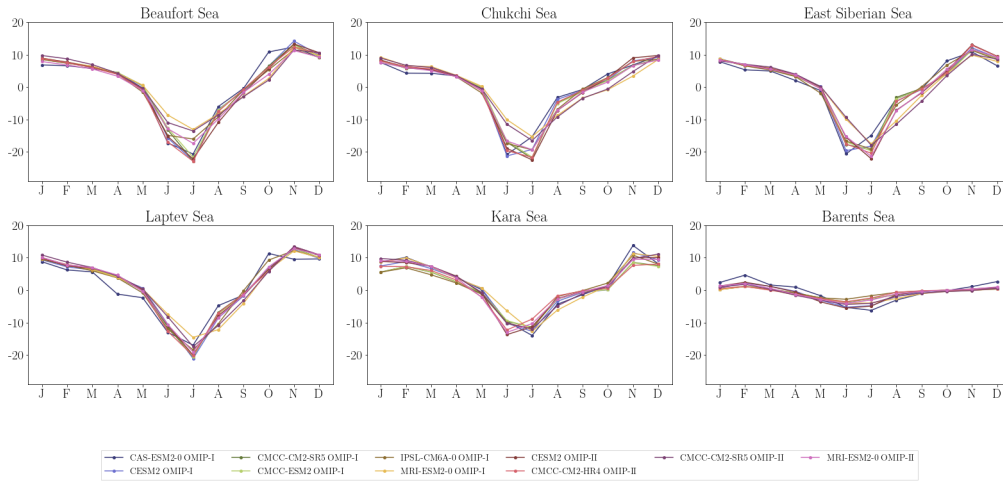

Figure A.4: Seasonal cycle of the salinity flux (ppt m/months) in the Beaufort (BeS), Chukchi (CS), East Siberian (ESS), Laptev (LS), Kara (KS), and Barents (BrS) Seas.
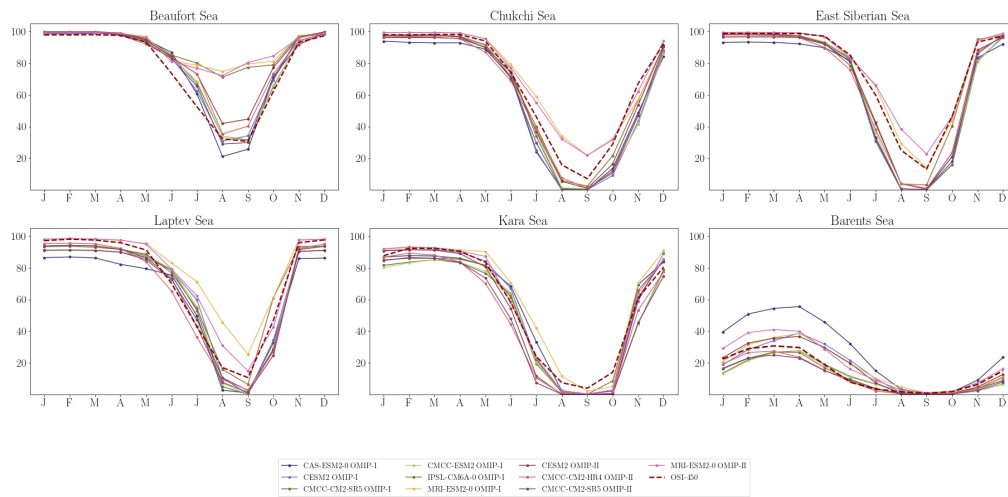

Figure A.5: Seasonal cycle of sea ice concentration in the Beaufort (BeS), Chukchi (CS), East Siberian (ESS), Laptev (LS), Kara (KS), and Barents (BrS) Seas. Red dashed-line corresponds to the observational data OSI-45 averaged from 2007 to 2011.

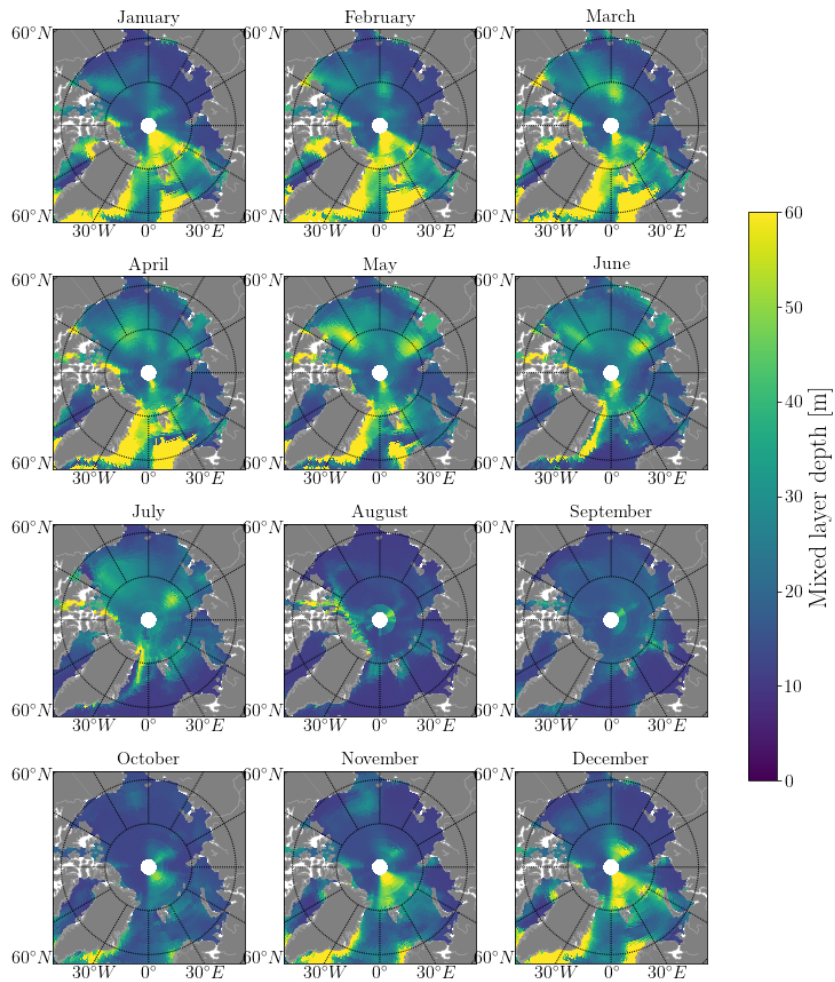On the ability of OMIP models to simulate the ocean mixed layer depth and its seasonal cycle in the Arctic Ocean

Figure A.6: MLD maps from the CAS-ESM2-0 OMIP-I model averaged during the years 2007-2009.

On the ability of OMIP models to simulate the ocean mixed layer depth and its seasonal cycle in the Arctic Ocean

References

Ardyna, M., Mundy, C.J., Mayot, N., Matthes, L.C., Oziel, L., Horvat, C., Leu, E., Assmy, P., Hill, V., Matrai, P.A., et al., 2020. Under-ice phytoplankton blooms: Shedding light on the "invisible" part of arctic primary production. Frontiers in Marine Science , 985.

Arrigo, K.R., Perovich, D.K., Pickart, R.S., Brown, Z.W., Van Dijken, G.L., Lowry, K.E., Mills, M.M., Palmer, M.A., Balch, W.M., Bahr, F., et al., 2012. Massive phytoplankton blooms under arctic sea ice. Science 336, 1408–1408.

Barthélemy, A., Fichefet, T., Goosse, H., Madec, G., 2015. Modeling the interplay between sea ice formation and the oceanic mixed layer: Limitations of simple brine rejection parameterizations. Ocean Modelling 86, 141–152.

Blanke, B., Delecluse, P., 1993. Variability of the tropical atlantic ocean simulated by a general circulation model with two different mixed-layer physics. Journal of Physical Oceanography 23, 1363–1388.

Boles, E., Provost, C., Garcon, V., Bertosio, C., Athanase, M., Koenig, Z., Sennéchael, N., 2020. Under-ice phytoplankton blooms in the central arctic ocean: Insights from the first biogeochemical iaoos platform drift in 2017. Journal of Geophysical Research: Oceans 125, e2019JC015608.

Boucher, O., Servonnat, J., Albright, A.L., Aumont, O., Balkanski, Y., Bastrikov, V., Bekki, S., Bonnet, R., Bony, S., Bopp, L., et al., 2020. Presentation and evaluation of the ipsl-cm6a-lr climate model. Journal of Advances in Modeling Earth Systems 12, e2019MS002010.

Canuto, V., Howard, A., Cheng, Y., Dubovikov, M., 2002. Ocean turbulence. part ii: Vertical diffusivities of momentum, heat, salt, mass, and passive scalars. Journal of Physical Oceanography 32, 240–264.

Canuto, V., Howard, A., Cheng, Y., Dubovikov, M.S., 2001. Ocean turbulence. part i: One-point closure model—momentum and heat vertical diffusivities. Journal of Physical Oceanography 31, 1413–1426.

Cassotta, S., Derksen, C., Ekaykin, A., Hollowed, A., Kofinas, G., MAckintosh, A., Melbourne-Thomas, J., Muelbert, M., Ottersen, G., Pritchard, H., et al., 2022. Special report on ocean and cryosphere in a changing chapter intergovernmental panel on climate change (ipcc), in: Chapter 3 Polar Issues. Cambridge University Press.

Cherchi, A., Fogli, P.G., Lovato, T., Peano, D., Iovino, D., Gualdi, S., Masina, S., Scoccimarro, E., Materia, S., Bellucci, A., et al., 2019. Global mean climate and main patterns of variability in the cmcc-cm2 coupled model. Journal of Advances in Modeling Earth Systems 11, 185–209.

Cole, S., Stadler, J., 2019. Deepening of the winter mixed layer in the canada basin, arctic ocean over 2006–2017. Journal of Geophysical Research: Oceans 124, 4618–4630.

Danabasoglu, G., Lamarque, J.F., Bacmeister, J., Bailey, D.A., DuVivier, A.K., Edwards, J., Emmons, L.K., Fasullo, J., Garcia, R., Gettelman, A., et al., 2020. The community earth system model version 2 (cesm2). Journal of Advances in Modeling Earth Systems 12, e2019MS001916.

Dong, X., Jin, J., Liu, H., Zhang, H., Zhang, M., Lin, P., Zeng, Q., Zhou, G., Yu, Y., Song, M., et al., 2021. Cas-esm2.0 model datasets for the cmip6 ocean model intercomparison project phase 1 (omip1). Advances in Atmospheric Sciences 38, 307–316.

Fournier, S., Lee, T., Wang, X., Armitage, T., Wang, O., Fukumori, I., Kwok, R., 2020. Sea surface salinity as a proxy for arctic ocean freshwater changes. Journal of Geophysical Research: Oceans 125, e2020JC016110.

Gettelman, A., Rood, R.B., 2016. Demystifying climate models: A users guide to earth system models. Springer Nature.

Goosse, H., Kay, J.E., Armour, K.C., Bodas-Salcedo, A., Chepfer, H., Docquier, D., Jonko, A., Kushner, P.J., Lecomte, O., Massonnet, F., et al., 2018. Quantifying climate feedbacks in polar regions. Nature communications 9, 1–13.

Griffies, S.M., Danabasoglu, G., Durack, P.J., Adcroft, A.J., Balaji, V., Böning, C.W., Chassignet, E.P., Curchitser, E., Deshayes, J., Drange, H., et al., 2016. Omip contribution to cmip6: Experimental and diagnostic protocol for the physical component of the ocean model intercomparison project. Geoscientific Model Development 9, 3231–3296.

Holte, J., Talley, L., 2009. A new algorithm for finding mixed layer depths with applications to argo data and subantarctic mode water formation. Journal of Atmospheric and Oceanic Technology 26, 1920–1939.

Horvat, C., Jones, D.R., Iams, S., Schroeder, D., Flocco, D., Feltham, D., 2017. The frequency and extent of sub-ice phytoplankton blooms in the arctic ocean. Science advances 3, e1601191.

Horvat, C., Tziperman, E., Campin, J.M., 2016. Interaction of sea ice floe size, ocean eddies, and sea ice melting. Geophysical Research Letters 43, 8083–8090.

Ilıcak, M., Drange, H., Wang, Q., Gerdes, R., Aksenov, Y., Bailey, D., Bentsen, M., Biastoch, A., Bozec, A., Böning, C., et al., 2016. An assessment of the arctic ocean in a suite of interannual core-ii simulations. part iii: Hydrography and fluxes. Ocean Modelling 100, 141–161.

Jackson, J., Williams, W., Carmack, E., 2012. Winter sea-ice melt in the canada basin, arctic ocean. Geophysical Research Letters 39.

Keen, A., Blockley, E., Bailey, D.A., Boldingh Debernard, J., Bushuk, M., Delhaye, S., Docquier, D., Feltham, D., Massonnet, F., O'Farrell, S., et al., 2021. An inter-comparison of the mass budget of the arctic sea ice in cmip6 models. The Cryosphere 15, 951–982.

Krishfield, R., Toole, J., Timmermans, M., 2008. Itp data processing procedures. Woods Hole Oceanographic Institution Tech. Rep 24.

Lavergne, T., Sørensen, A.M., Kern, S., Tonboe, R., Notz, D., Aaboe, S., Bell, L., Dybkjær, G., Eastwood, S., Gabarro, C., et al., 2019. Version 2 of the eumetsat osi saf and esa cci sea-ice concentration climate data records. The Cryosphere 13, 49–78.

Levitus, S., 1982. Climatological atlas of the world ocean. volume 13. US Department of Commerce, National Oceanic and Atmospheric Administration.

Li, Q., Webb, A., Fox-Kemper, B., Craig, A., Danabasoglu, G., Large, W.G., Vertenstein, M., 2016. Langmuir mixing effects on global climate: Wavewatch iii in cesm. Ocean Modelling 103, 145–160.

Lin, X., Massonnet, F., Fichefet, T., Vancoppenolle, M., 2022. Impact of atmospheric forcing uncertainties on arctic and antarctic sea ice simulation in cmip6 omip. The Cryosphere Discussions , 1–40.

Lovato, T., Peano, D., Butenschön, M., Materia, S., Iovino, D., Scoccimarro, E., Fogli, P.G., Cherchi, A., Bellucci, A., Gualdi, S., et al., 2022. Cmip6 simulations with the cmcc earth system model (cmcc-esm2). Journal of Advances in Modeling Earth Systems 14, e2021MS002814.

Martinson, D.G., 1990. Evolution of the southern ocean winter mixed layer and sea ice: Open ocean deepwater formation and ventilation. Journal of Geophysical Research: Oceans 95, 11641–11654.

McPhee, M., 2008. Air-ice-ocean interaction: Turbulent ocean boundary layer exchange processes. Springer Science & Business Media.

Meredith, M., Sommerkorn, M., Cassota, S., Derksen, C., Ekaykin, A., Hollowed, A., Kofinas, G., Mackintosh, A., Melbourne-Thomas, J., Muelbert, M., et al., 2019. Polar regions. chapter 3, ipcc special report on the ocean and cryosphere in a changing climate .

On the ability of OMIP models to simulate the ocean mixed layer depth and its seasonal cycle in the Arctic Ocean

Mizobata, K., Shimada, K., 2012. East–west asymmetry in surface mixed layer and ocean heat content in the pacific sector of the arctic ocean derived from amsr-e sea surface temperature. Deep Sea Research Part II: Topical Studies in Oceanography 77, 62–69.

Nummelin, A., Ilicak, M., Li, C., Smedsrud, L.H., 2016. Consequences of future increased arctic runoff on arctic ocean stratification, circulation, and sea ice cover. Journal of Geophysical Research: Oceans 121, 617–637.

Peralta-Ferriz, C., Woodgate, R.A., 2015. Seasonal and interannual variability of pan-arctic surface mixed layer properties from 1979 to 2012 from hydrographic data, and the dominance of stratification for multiyear mixed layer depth shoaling. Progress in Oceanography 134, 19–53.

Perovich, D.K., Richter-Menge, J.A., 2009. Loss of sea ice in the arctic. Annual review of marine science 1, 417–441.

Polyakov, I., Pnyushkov, A., Rember, R., Padman, L., Carmack, E., Jackson, J., 2013. Winter convection transports atlantic water heat to the surface layer in the eastern arctic ocean. Journal of Physical Oceanography 43, 2142–2155.

Rippeth, T., Fine, E., 2022. Turbulent mixing in a changing arctic ocean. Oceanography .

Schmidtko, S., Johnson, G.C., Lyman, J.M., 2013. Mimoc: A global monthly isopycnal upper-ocean climatology with mixed layers. Journal of Geophysical Research: Oceans 118, 1658–1672.

Shu, Q., Wang, Q., Guo, C., Song, Z., Wang, S., He, Y., Qiao, F., 2022. Arctic ocean simulations in the cmip6 ocean model intercomparison project (omip). Geoscientific Model Development Discussions , 1–34.

Stranne, C., Mayer, L., Jakobsson, M., Weidner, E., Jerram, K., Weber, T., Anderson, L., Nilsson, J., Björk, G., Gårdfeldt, K., 2018. Acoustic mapping of mixed layer depth. Ocean Science 14, 503–514.

Timmermans, M.L., Cole, S., Toole, J., 2012. Horizontal density structure and restratification of the arctic ocean surface layer. Journal of Physical Oceanography 42, 659–668.

Timmermans, M.L., Marshall, J., 2020. Understanding arctic ocean circulation: A review of ocean dynamics in a changing climate. Journal of Geophysical Research: Oceans 125, e2018JC014378.

Toole, J., Krishfield, R., Timmermans, M., Proshutinsky, A., 2011. The ice-tethered profiler: Argo of the arctic. Oceanography 24, 126–135.

Treguier, A., de Boyer Montégut, C., Bozec, A., Chassignet, E., Fox-Kemper, B., Hogg, A., Iovino, D., Kiss, A., Le Sommer, J., Li, Y., et al., 2023. The mixed layer depth in the ocean model intercomparison project (omip): Impact of resolving mesoscale eddies. EGUsphere .

Tsujino, H., Urakawa, L.S., Griffies, S.M., Danabasoglu, G., Adcroft, A.J., Amaral, A.E., Arsouze, T., Bentsen, M., Bernardello, R., Böning, C.W., et al., 2020. Evaluation of global ocean–sea-ice model simulations based on the experimental protocols of the ocean model intercomparison project phase 2 (omip-2). Geoscientific Model Development 13, 3643–3708.

Umlauf, L., Burchard, H., 2003. A generic length-scale equation for geophysical turbulence models. Journal of Marine Research 61, 235–265.

Watts, M., Maslowski, W., Lee, Y.J., Kinney, J., Osinski, R., 2021. A spatial evaluation of arctic sea ice and regional limitations in cmip6 historical simulations. Journal of Climate , 1–54.

Yukimoto, S., Kawai, H., Koshiro, T., Oshima, N., Yoshida, K., Urakawa, S., Tsujino, H., Deushi, M., Tanaka, T., Hosaka, M., et al., 2019. The meteorological research institute earth system model version 2.0, mri-esm2. 0: Description and basic evaluation of the physical component. Journal of the Meteorological Society of Japan. Ser. II .

CRediT authorship contribution statement
S Allende: Conceptualization of this study, Methodology, Formal analysis, Writing - Original Draft, Visualization.
T Fichefet: Conceptualization of this study, Writing - Review & Editing .
H Goosse: Conceptualization of this study,Writing - Review & Editing .
AM Treguier: Conceptualization of this study, Writing - Review & Editing .

Declaration of interests

☒ The authors declare that they have no known competing financial interests or personal relationships that could have appeared to influence the work reported in this paper.

☐ The authors declare the following financial interests/personal relationships which may be considered as potential competing interests: